2

High Resolution Mass Spectrometry Using FTICR and *Orbitrap* Instruments

Paulo J. Amorim Madeira, Pedro A. Alves and Carlos M. Borges
Centro de Química e Bioquímica, Departamento de Química e Bioquímica, Faculdade de Ciências da Universidade de Lisboa
Portugal

1. Introduction

From the 1950s to the present, mass spectrometry has evolved tremendously. The pioneering mass spectrometrist had a home-built naked instrument, typically a magnetic sector instrument with electron ionisation. Nowadays, highly automated commercial systems, able to produce thousands of spectra per day, are now concealed in a "black box", a nicely designed and beautifully coloured unit resembling more an espresso machine or a tumble dryer than a mass spectrometer.

Mass spectrometry (MS) is probably the most versatile and comprehensive analytical technique currently available in the chemists and biochemists' arsenal. Mass spectrometry precisely measures the molecular masses of individual compounds by converting them into charged ions and analysing them in what is called a mass analyser. This is the simplest, but somewhat reductionist, definition of mass spectrometry. The days of the simple determination of the *m/z* ratio of an organic compound are over, today mass spectrometry can be used to determine molecular structures, to study reaction dynamics and ion chemistry, provides thermochemical and physical properties such as ionisation and appearance energies, reaction enthalpies, proton and ion affinities, gas-phase acidities, and so on.

Mass spectrometry is so versatile that even several areas of physics, pharmaceutical sciences, archaeology, forensic and environmental sciences, just to state a few, have benefited from the advances in this instrumental technique.

The history of mass spectrometry starts in 1898 with the work of Wien, who demonstrated that canal rays could be deflected by passing them through superimposed parallel electric and magnetic fields. Nevertheless, its birth can be credited to Sir J. J. Thomson, Cavendish Laboratory of the University of Cambridge, through his work on the analysis of negatively and positively charged cathode rays with a parabola mass spectrograph, the great grand-father of the modern mass spectrometers. (Thomson 1897; Thomson 1907) In the next two decades, the developments of mass spectrometry continued by renowned physicists like Aston, (Aston 1919) Dempster, (Dempster 1918) Bainbridge, (Bainbridge 1932; Bainbridge and Jordan 1936) and Nier. (Nier 1940; Johnson and Nier 1953)

In the 1940s, chemists recognised the great potential of mass spectrometry as an analytical tool, and applied it to monitor petroleum refinement processes. The first commercial mass spectrometer became available in 1943 through the Consolidated Engineering Corporation. The principles of time-of-flight (TOF) and ion cyclotron resonance (ICR) were introduced in 1946 and 1949, respectively. (Sommer, Thomas et al. 1951; Wolff and Stephens 1953)

Applications to organic chemistry started to appear in the 1950s and exploded during the 1960s and 1970s. Double-focusing high-resolution mass spectrometers, which became available in the early 1950s, paved the way for accurate mass measurements. The quadrupole mass analyser and the ion trap were described by Wolfgang Paul and co-workers in 1953. (Paul 1990) The development of gas chromatography/mass spectrometry (GC/MS) in the 1960s marked the beginning of the analysis of seemingly complex mixtures by mass spectrometry. (Ryhage 2002; Watson and Biemann 2002) The 1960s also witnessed the development of tandem mass spectrometry and collision-induced decomposition, (Jennings 1968) being a breakthrough in structural and quantitative analysis, as well as in the development of soft ionisation techniques such as chemical ionisation. (Munson and Field 1966)

By the 1960s, mass spectrometry had become a standard analytical tool in the analysis of organic compounds. Its application to the biosciences, however, was lacking due to the inexistence of suitable methods to ionise fragile and non-volatile compounds of biological origin. During the 1980s the range of applications in the field of the biosciences increased "exponentially" with the development of softer ionisation methods. These included fast atom bombardment (FAB) in 1981, (Barber, Bordoli et al. 1981) electrospray ionisation (ESI) in 1984-1988, (Fenn, Mann et al. 1989) and matrix-assisted laser desorption/ionisation (MALDI) in 1988. (Karas and Hillenkamp 2002) With the development of the last two methods, ESI and MALDI, the upper mass range was extended beyond 100 kDa and had an enormous impact on the use of mass spectrometry in biology and life sciences. This impact was recognised in 2002 when John Fenn (for his work on ESI) and Koichi Tanaka (for demonstrating that high molecular mass proteins could be ionised using laser desorption) were awarded with the Nobel Prize in Chemistry.

Concurrent with the development of ionisation methods, several innovations in mass analyser technology, such as the introduction of high-field and superfast magnets, as well as the improvements in the TOF and Fourier transform ion cyclotron resonance (FTICR) enhanced the sensitivity and the upper mass range. The new millennium brought us two new types of ion traps, the orbitrap which was invented by Makarov (Makarov 2000) and the linear quadrupole ion trap (LIT) which was developed by Hager. (Hager 2002)

The coupling of high-performance liquid chromatography (HPLC) with mass spectrometry was first demonstrated in the 1970s (Dass 2007); nevertheless, it was with the development and commercialisation of atmospheric pressure ionisation sources (ESI, APCI) that for the first time the combination of liquid chromatography and mass spectrometry entered the realm of routine analysis. (Voyksner 1997; Covey, Huang et al. 2002; Whitehouse, Dreyer et al. 2002; Rodrigues, Taylor et al. 2007)

Generally, a mass spectrometer is composed of five components (Fig. 1): inlet system, ion source, mass analyser, ion detector, and data system.

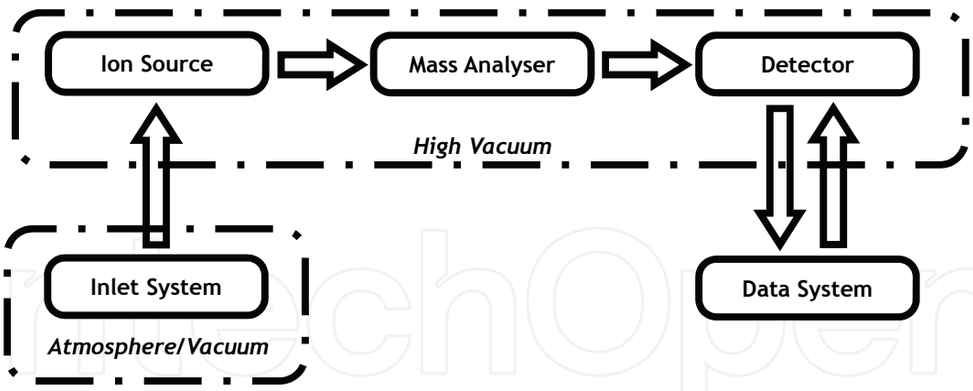

Fig. 1. Diagram of the major components common to all typical modern mass spectrometers

Samples are introduced in the mass spectrometer and transferred into the gas phase through the inlet system that could be at atmospheric pressure or under vacuum. In the ion source, the gas-phase analytes are ionised and transferred into the mass analyser where they are separated according to their mass-to-charge ratios (*m/z*). Ion detection can be accomplished by electron multiplier systems that enable *m/z* and abundance to be measured and displayed by means of an electric signal perceived by the data system, which also controls the equipment. All mass spectrometers are equipped with a vacuum system in order to maintain the low pressure (high vacuum) required for operation. This high vacuum is necessary to allow ions to reach the detector without undergoing collisions with other gaseous molecules. In fact, collisions would produce a deviation of the trajectory and the ion would lose its charge against the walls of the instrument. On the other hand, a relatively high pressure environment could facilitate the occurrence of ion-molecule reactions that would increase the complexity of the spectrum. In some experiments the pressure in the source region or in a part of the mass spectrometer is intentionally increased to study ion-molecule reactions or to perform collision-induced dissociations. The high vacuum is maintained using mechanical pumps in conjunction with turbomolecular, diffusion or cryogenic pumps. The mechanical pumps allow a vacuum of about 10^{-3} torr to be obtained. Once this vacuum is achieved the operation of the remainder of the vacuum system allows a vacuum as high as 10^{-10} torr to be reached.

2. Fourier transforms in mass spectrometry

In the following sections we will briefly describe two types of mass analysers that employ Fourier transforms to determine *m/z* ratios. We will describe the Fourier Transform Ion Cyclotron Resonance mass spectrometer (FTICR MS) and the *Orbitrap* in sections 2.1 and 2.2, respectively. The basic aspects of each mass analyser will be dealt with; nevertheless, the interested reader is encouraged to seek more information in the literature. For example, in the case of FTICR mass spectrometry several reviews (Marshall, Hendrickson et al. 1998; Zhang, Rempel et al. 2005) and books are available. (Marshall and Verdun 1990; Gross 2004; Dass 2007; Hoffmann and Stroobant 2007) For the *Orbitrap*, the operation principles are well described in the papers published by Makarov, its inventor, (Makarov 2000; Hu, Noll et al. 2005; Makarov, Denisov et al. 2006) as well as by other authors, (Perry, Cooks et al. 2008) and in the more recent editions of some mass spectrometry textbooks. (Dass 2007; Hoffmann and Stroobant 2007)

2.1 Fourier transform ion cyclotron resonance mass spectrometry (FTICR MS)

The theory of cyclotron resonance was developed in the 1930s by Lawrence (1951 Nobel Prize in Physics). Lawrence built the first cyclotron accelerator to study the fundamental properties of the atom. Subsequently, Penning devised the first trap for charged particles by using a combination of static electric and magnetic fields to confine electrons. (Vartanian, Anderson et al. 1995) In the 1950s the principle of ion cyclotron resonance was first incorporated into a mass spectrometer, called the omegatron, by Sommer and co-workers, who successfully applied the concept of cyclotron resonance to determine the charge-to-mass ratio of the proton. (Sommer, Thomas et al. 1951) Major improvements in ICR awaited McIver's introduction of the trapped ion cell. Unlike the conventional drift cell, the trapped ion cell allowed for ion formation, manipulation and detection to occur within the same volume in space. The trapped ion cell differed from previous ICR cell designs by the inclusion of "trapping" electrodes. By applying small voltages to these electrodes, McIver was able to trap ions for 1-2 ms (approximately 100 times that of the drift cell). These advantages led to a much greater dynamic range, sensitivity and mass resolution. More importantly, the extended trapping capability of the McIver cell was a prerequisite for the FTICR detection technique invented by Comisarow and Marshall later that decade. In the second half of the 1970s, Comisarow and Marshall adapted Fourier transform methods to ICR spectrometry and built the first FTICR-MS instrument. (Comisarow and Marshall 1974; Marshall, Comisarow et al. 1979) Since then, FTICR-MS has matured into a state-of-the-art high-resolution mass spectrometry instrument for the analysis of a wide variety of compounds (biological or not).

All FTICR-MS systems have in common five main components: a magnet (nowadays usually a superconducting magnet); analyser cell (placed in the strong magnetic field created by the magnet); ultra-high vacuum system, and ion source (Fig. 2); and a sophisticated data system (many of the components in the data system are similar to those used in NMR).

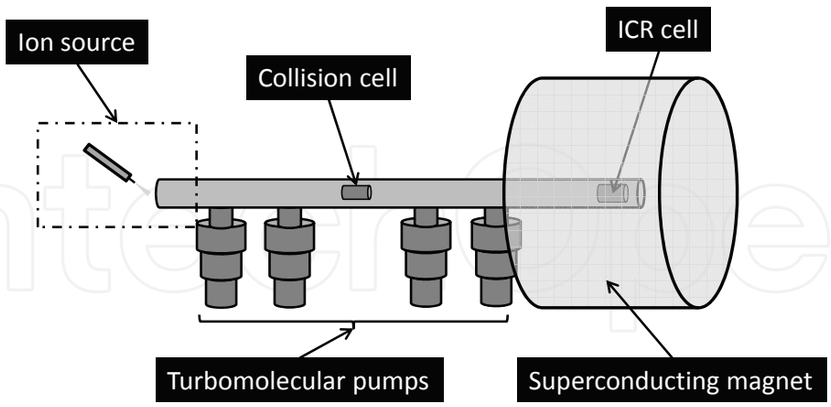

Fig. 2. Schematic representation of an FTICR mass spectrometer. Note that not all components are present in this scheme, for example, the ion optics is not presented, nor the rotary vacuum pumps that are needed for the proper functioning of the turbomolecular pumps

In this section, we shall not discuss the magnet, vacuum and data systems, and focus on the ICR cell, which is the heart of the FTICR-MS instrument. It is here that the ions are stored, mass analysed and detected.

Inside the FTICR cell an ion has three natural motions: the cyclotron, the trapping and the magnetron motions. The nature of each motion will be briefly explained in the following paragraphs.

Many fundamental aspects of FTICR can be understood from very simple idealised models:

- Ion cyclotron frequency, radius, velocity and energy, as a function of ion mass, ion charge and magnetic field strength, follow directly from the motion of an ion in a spatially uniform static magnetic field.
- Ion cyclotron motion may be rendered coherent (and thus observable) by the application of a spatially uniform RF electric field (excitation) at the same frequency as the ion cyclotron frequency. The ICR signal results from induction of an oscillating "image" charge on two conductive infinitely extended opposed parallel electrodes. A frequency-domain spectrum is obtained by Fourier transformation of the digitised ICR signal.
- Confinement of ions by application of a three-dimensional axial quadrupolar DC electric field shifts the ion cyclotron frequency, whereas excitation and detection remain essentially linear, but with a reduced proportionality constant.
- Collisions broaden the ICR signal in a simple way, and actually make it possible to cool and compress an ion packet for improved detection.
- Although FTICR-MS has been coupled to virtually every type of ion source, most ion sources work best outside the magnet. Thus, several methods have been developed to guide the externally generated ions into the ion trap inside a high-field magnet.
- The above features may be combined in various experimental "event sequences" to perform tandem-in-time mass spectrometry (MS/MS or MS^n).

Cyclotron motion

An ion moving in the presence of a uniform electric and magnetic fields, E and B, is subjected to a Lorentz force given by equation 1, where m, q and v are the mass, charge and velocity.

$$F = ma = m\frac{dv}{dt} = qE + qvB \tag{1}$$

Let us now consider only the presence of the magnetic field, B. If the ion maintains constant speed (i.e. no collisions), then the magnetic field bends the ion path into a circle of radius r, the cyclotron motion (Fig. 2).

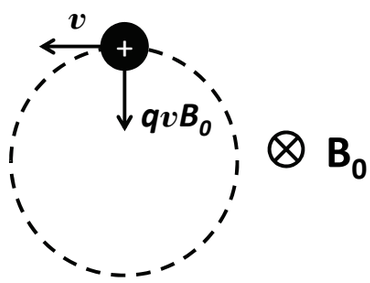

Fig. 2. Ion cyclotron motion for a positive or negative ion due to the presence of a magnetic field (B) perpendicular to the plane of the paper

The angular acceleration and angular velocity, ω, are defined by equations 2 and 3.

$$\frac{dv}{dt} = \frac{{v_{xy}}^2}{r} \tag{2}$$

$$\omega = \frac{v_{xy}}{r} \tag{3}$$

Substituting these terms in equation 1 we obtain[1]

$$\omega_c = \frac{qB}{m} \tag{4}$$

Equation 4 is the celebrated "cyclotron" equation that relates the cyclotron frequency, ω_c, with the mass and charge of the ion. It is clear that for a given *m/z* all ions have the same ICR frequency independent of their initial velocity; hence, energy focussing is not required to precisely determine the *m/z* ratio of an ion.

Several useful conclusions arise from the cyclotron equation (eq. 4). Considering an *m/z* range of 10 to 100 000, the frequencies lie between a few kHz and a few MHz (Fig. 3), which is a very convenient range for commercially available electronics.

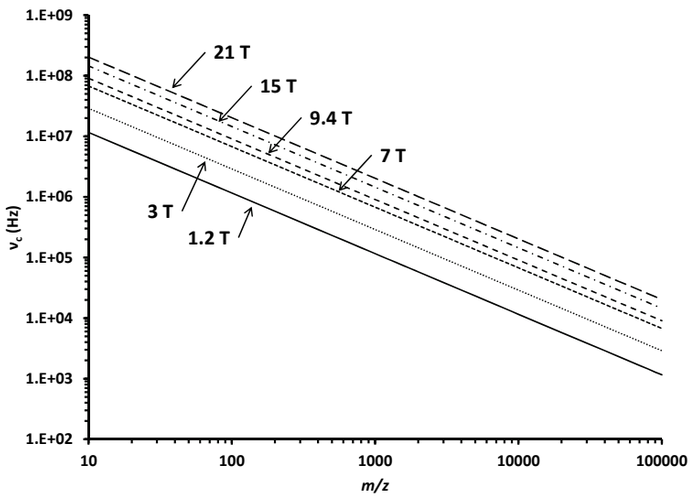

Fig. 3. ICR orbital frequency (for ions in the *m/z* range between 10 and 100 000) as a function of *m/z* at 1.2 T, 3 T, 7 T, 9.4 T, 15 T (highest magnetic field strength commercially available) and 21 T (highest magnetic field strength magnet under development at the National High Magnetic Field Laboratory in the USA)

The first derivative of the cyclotron equation with respect to *m* gives equation 5, which allows us to conclude that frequency resolution and mass resolution are essentially the same (apart from the minus sign).

[1] All of the equations will be presented in S.I. units. To convert, for example, m/q to m/z the reader should take into account that q = z×e, where z is in multiples of elementary charge (e = 1.602×10-19 C) and m is in atomic mass units (1u = 1.660×10-27 kg).

$$\frac{d\omega_c}{dm} = -\frac{qB}{m^2} = -\frac{\omega_c}{m} \Leftrightarrow \frac{\omega_c}{d\omega_c} = -\frac{m}{dm} \tag{5}$$

Finally, considering that the average kinetic energy of an ion with velocity v_{xy} in equilibrium with its surroundings at a temperature T (in K) is given by equation 6 (where k is the Boltzmann's constant) and that the ion cyclotron orbital radius, r, is given by equation 7 (derived from equation 3).

$$\frac{1}{2}m\langle {v_{xy}}^2 \rangle \cong kT \Leftrightarrow v_{xy} = \sqrt{2kT/m} \tag{6}$$

$$r = \frac{mv_{xy}}{qB_0} \tag{7}$$

Substituting v_{xy} in equation 7 we obtain an expression that relates the ion cyclotron orbital radius as a function of *m/z* ratio (equation 8).

$$r = \frac{1}{qB_0}\sqrt{2mkT} \tag{8}$$

Considering T=298 K and various magnetic field strengths, we can construct a graphical representation of r as a function of *m/z* (Fig. 4). This representation allows us to conclude that even large ions are confined by the magnetic field to a small orbital radius. For example, a "modest" superconducting magnet of 3 T confines an ion with *m/z* 2000 to an orbit with a radius smaller than 0.5 mm.

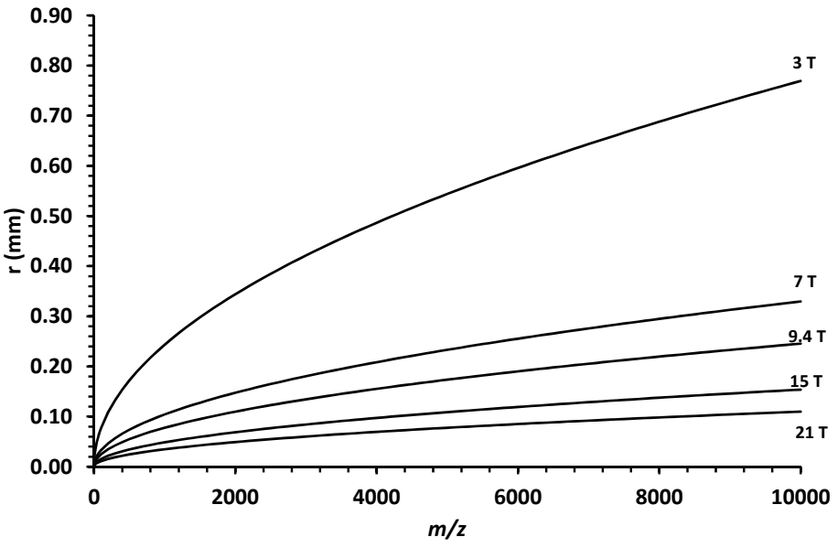

Fig. 4. ICR orbital radius, r, vs. *m/z* ratio at 298K and 3 T, 7 T, 9.4 T, 15 T and 21 T

It is also possible to relate the kinetic energy of a trapped ion with its orbital radius by rearranging equation 7 (equation 9). A graphical representation of the ion's kinetic energy as a function of the orbital radius, depicted in Fig. 5 for a singly charged ion at *m/z* 400, reveals that ions can be heated to high kinetic energies even in a relatively small container.

$$E_k = \frac{r^2 q^2 {B_0}^2}{2m} \tag{9}$$

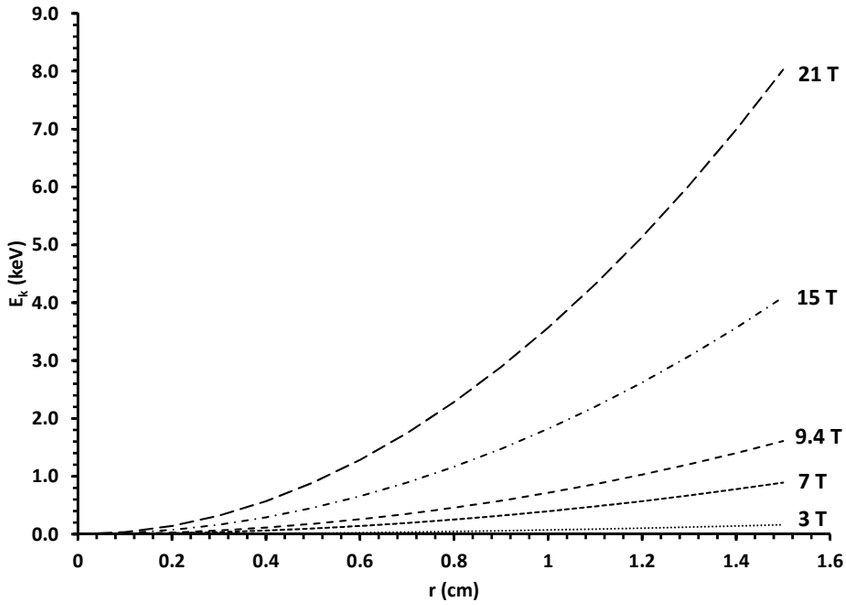

Fig. 5. Ion kinetic energy as a function of the ICR orbital radius (singly charged ion at *m/z* 400)

Trapping motion

The static magnetic field effectively confines ions in the xy plane; nevertheless, ions are still free to escape along the z-axis. To prevent this, a small electrostatic potential (equation 10), usually ≈ 1 V, is applied to the trapping electrodes (positioned at $z = \pm d/2$ from the center of the ion trap). (Vartanian, Anderson et al. 1995)

$$V(z) \cong \frac{V_t}{2} + \frac{k' z^2}{2} \tag{10}$$

where k′ is a constant.

The trapping electric field can be obtained by the negative gradient with respect to z of the electrostatic potential (equation 11).

$$E(z) = -\frac{dV(z)}{dz} = -k' z \tag{11}$$

This electric field subjects the trapped ion to a force, $F(z)$, given by equation 12

$$F(z) = -\frac{d^2 z}{dz^2} = -qk' z \tag{12}$$

Equation 12 resembles the harmonic oscillator equation; hence, ions trapped in a quadratic z-potential must oscillate back and forth along the z-direction at a natural trapping

frequency, the so-called trapping motion (or trapping oscillation). The trapping frequency, ω_T, and the k' constant are defined by equations 13 and 14, respectively.

$$\omega_T = \sqrt{\frac{k'q}{m}} \tag{13}$$

$$k' = \frac{4V_T}{d^2} \tag{14}$$

Substituting k' in equation 13 we obtain

$$\omega_T = \frac{2}{d}\sqrt{\frac{qV_T}{m}} \tag{15}$$

In general, the trapping frequency is much smaller than the ICR frequency so it is not detected.

Magnetron motion

The combination of the magnetic field and the radial component of the electric field created by the trapping potential induce a third motion: the magnetron rotation. The magnetron frequency (equation 16), ω_m, is independent of both the mass and charge of the ion. Nevertheless, it is proportional to the trapping voltage (V_T) and the cell geometry factor (α) and inversely proportional to the cell edge length (a) and the magnetic field strength (B). (Vartanian, Anderson et al. 1995)

$$\omega_m = \frac{2\alpha V_T}{a^2 B} \tag{16}$$

Cyclotron + Trapping + Magnetron Motions

The three natural ion motions (cyclotron rotation, magnetron rotation and trapping oscillation) are depicted in Fig. 6. As mentioned earlier, the magnetron and trapping frequencies are usually much smaller than the cyclotron frequency and generally are not detected. Nevertheless, several reviews on the subject of ion trajectories inside the ICR cell and their influence on the cyclotron frequency were published over the years, e.g. the one by Vartanian *et al.* (Vartanian, Anderson et al. 1995)

Excitation and detection of an ICR signal

Ion cyclotron motion does not by itself generate an observable electric signal. When the ion packets enter the ICR cell, their ion cyclotron orbits are centred on the z-axis (i.e. they are too small to be detected) and must be made spatially coherent by moving them away from the centre of the cell. For that purpose excitation is needed and this is achieved by applying a spatially uniform electric field oscillating at or near the cyclotron frequency of ions of a particular *m/z* range.

Excitation is used in three ways in FTICR-MS:

- To accelerate ions coherently to a larger (and thus detectable) orbital radius – Fig. 7 a);

- To increase ion kinetic energy above the threshold for ion dissociation and/or ion-molecule reaction – Fig. 7 b);
- To accelerate ions to a cyclotron radius larger than the radius of the ion trap, so that ions are removed from the instrument – Fig. 7 c).

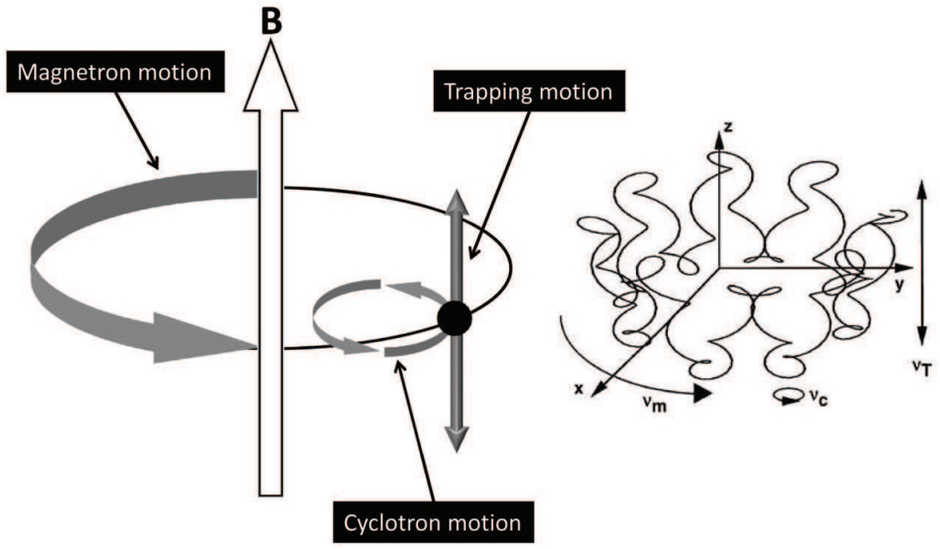

Fig. 6. Schematic representation of the three natural motions of an ion confined in an ICR cell and the resulting ion trajectory shape

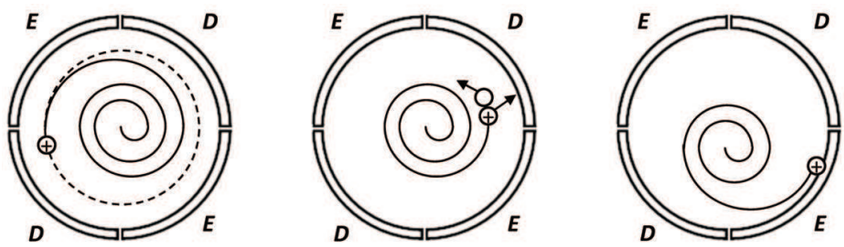

(a) (b) (c)

Fig. 7. Ion cyclotron excitation uses: a) acceleration of ions to larger orbital radius for detection; b) acceleration of ions to induce ion dissociation or ion-molecule reactions; c) removal of unwanted ions from the ICR cell. (*E* – Excitation electrode, *D* – Detection electrode)

In this chapter we will focus on the detection; the other two ways of using excitation (to increase the ion's kinetic energy and to remove undesired ions from the instrument) will not be addressed in this chapter. Nevertheless, more information can be obtained in a review by Marshall and co-workers. (Marshall, Hendrickson et al. 1998)

Spatial coherence is created by applying an oscillating resonant, $\omega = \omega_c$, phase-coherent electric field excitation *E (t)* (equation 17).

$$E(t) = E_0 \cos \omega t \, j \tag{17}$$

This linearly-polarised electric field can be decomposed into two counter-rotating components, $E(t)=E_L(t)+E_R(t)$ (equations 18 and 19).

$$E_L(t) = \frac{E_0}{2}\cos\omega t\,\boldsymbol{j} + \frac{E_0}{2}\sin\omega t\,\boldsymbol{i} \tag{18}$$

$$E_R(t) = \frac{E_0}{2}\cos\omega t\,\boldsymbol{j} - \frac{E_0}{2}\sin\omega t\,\boldsymbol{i} \tag{19}$$

With the excitation the ion speeds up and its radius increases linearly with time and the rate of power absorption is given by equation 20. (Marshall, Hendrickson et al. 1998)

$$A(t_{excite}) = \frac{{E_0}^2 q^2 t_{excite}}{4m} \tag{20}$$

The integration of equation 20 from *t=0* to $t=t_{excite}$ yields the total energy absorbed during the excitation period and assuming a complete conversion into kinetic energy we obtain

$$\frac{m{\omega_c}^2 r^2}{2} = \int_0^{t_{excite}} A(t)\,dt = \frac{{E_0}^2 q^2 (t_{excite})^2}{8m} \tag{21}$$

Substituting the cyclotron equation (equation 4) in equation 21 we obtain an expression that relates the radius with the excitation electric field and the excitation time.

$$r = \frac{E_0 t_{excite}}{2B_0} \tag{22}$$

An interesting conclusion arises from equation 22 in that the orbital radius of the excited ions is independent of the *m/z* ratio, which means that ions of different *m/z* ratios can be excited to the same ICR orbital radius.

The detection of the ions occurs as the ion packets pass two detector plates. As the ion packets have past these plates, charge moves within the detection circuit to counteract the proximity of the ions. The potential change (voltage) between the detection plates can be measured as a function of time and it is from here that the raw data is obtained. It should be noted that the ions repeatedly pass the detector plates for the duration of the acquisition, as non-destructive detection is employed. The magnitude of the signal is proportional to the total charge and to the proximity of the ions to the detection plates (orbital radius), and is independent of magnetic field strength. The raw data will represent the detections of all the ions at the same time, with their different cyclotron frequencies. It is therefore necessary to extract data concerning the different ion packets. This is done through the usage of a mathematical procedure known as Fourier transform (FT) where frequency information is obtained from time-domain data. Fig. 8 illustrates the process of obtaining a mass spectrum from the time-domain data through Fourier transform, conversion to *m/z* and calibration.

Unlike other mass spectrometers (e.g. sector instruments, time-of-flight, quadrupole) where mass analysis and ion detection are spatially separated events, in FTICR all analytical steps are made on the same spatial place but separated in time. Fig. 9 shows a typical sequence of events for a tandem mass spectrometry experiment performed in a FTICR mass spectrometer. Before ion introduction, the ICR cell is emptied with a quench pulse. After the ions have been introduced into the cell a significant amount of time is required for the ion selection, dissociation, excitation, detection, time-domain data storage and Fourier

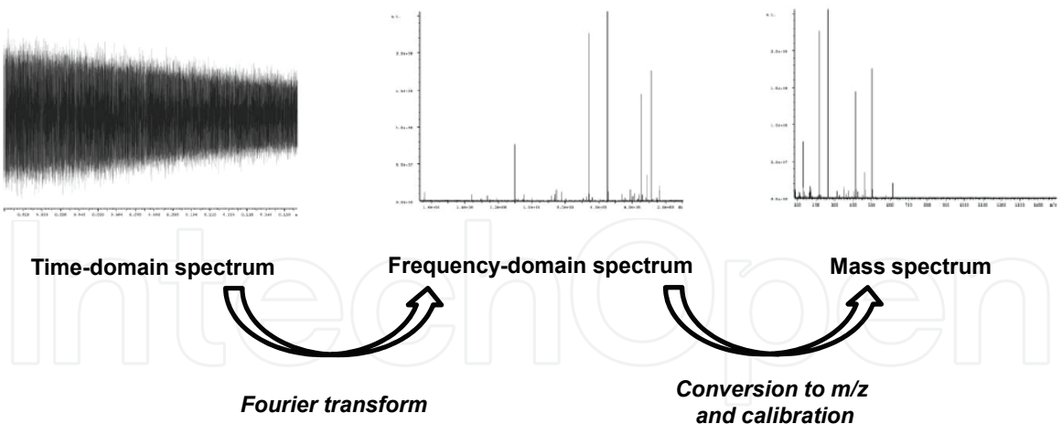

Fig. 8. Illustration of the processing of raw data. A Fourier transform is performed on time-domain data to convert it to the frequency-domain, and the resulting spectrum is then calibrated to *m/z* values

transformation events before the next experiment (i.e. sequence) is started. The time involved in the events that follow ion introduction, greatly depends on the instrument used and on the type of experiment (for example, the acquisition of a normal full scan mass spectrum will take less time than other mass spectra since the ion selection and dissociation steps will not be performed). (Heeren, Kleinnijenhuis et al. 2004)

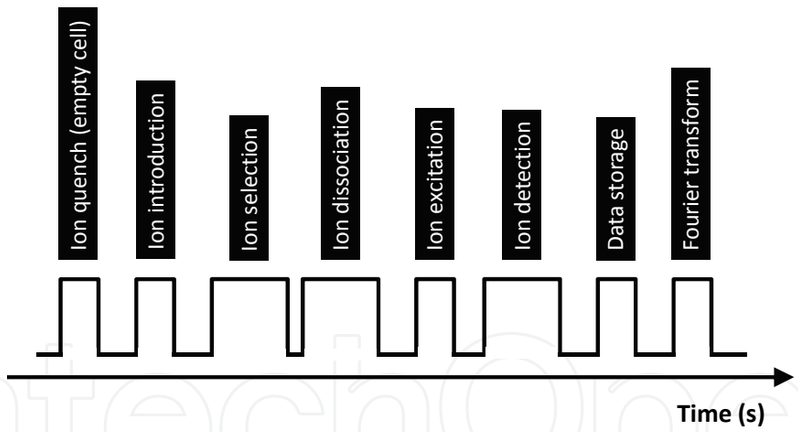

Fig. 9. Example for a tandem mass spectrometry sequence performed in a FTICR mass spectrometer. The sequence shows the order of the different time-separated analytical steps

2.2 Orbitrap mass spectrometry

The new millennium introduced a "new" mass analyser in the field of mass spectrometry that had not been stirred up since the first principles of FT-ICR. The *Orbitrap* (Fig. 10) is an ion trap that operates based only on an electrostatic field, by radially trapping ions about a central spindle electrode. An outer barrel-like electrode is coaxial with the inner spindle-like electrode and *m/z* values are measured from the frequency of harmonic ion oscillations along the axis of the electric field. This axial frequency is independent of the energy and spatial distribution of the ions. Ion frequencies are measured non-destructively by

acquisition of time-domain image current transients, with subsequent fast Fourier transforms (FFT) being used to obtain the mass spectra. (Hu, Noll et al. 2005)

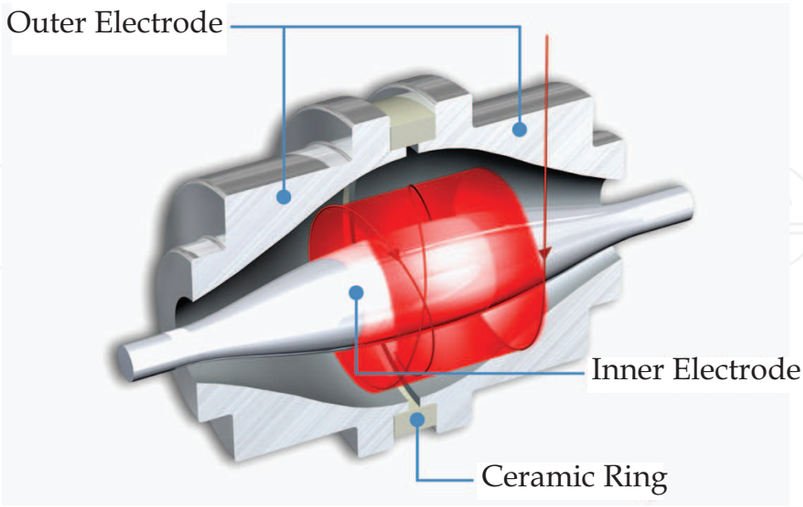

Fig. 10. *Orbitrap* mass analyser. Ions are captured in a quadrologarithmic electrostatic field. An outer electrode enclosing a central spindle electrode consists of two halves separated by a dielectric material. The image current of ions moving as concentric rings along the central electrode is picked up by the outer electrode sections. Image kindly supplied by Thermo Fisher Scientific

Features of the *Orbitrap* at its present stage of development include high mass resolution (up to 150 000), large space charge capacity, high mass accuracy (2–5 ppm), a mass/charge range of at least 6000, and dynamic range greater than 10^3. The current commercially available *Orbitrap* systems are equipped with several features that increase the range of applications. Fig. 11 depicts a hybrid ion trap-*Orbitrap* mass spectrometer equipped with an Electron Transfer Dissociation (ETD) module. ETD is the ion trap equivalent to Electron Capture Dissociation (a very popular fragmentation technique used in FTICR mass spectrometers)

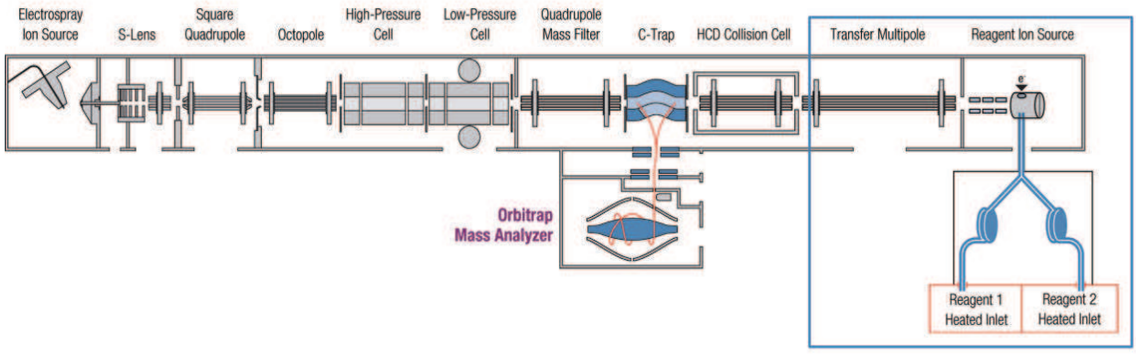

Fig. 11. Schematic representation of a hybrid ion trap-*Orbitrap* mass spectrometer. The main parts of a commercially available instrument are annotated on the diagram. The blue box highlights an optional ETD module which further extends the versatility of the system. Image kindly supplied by Thermo Fisher Scientific

that enables, for example, the probing of post-translational modifications of proteins. (Jung, Pasini et al. 2010)

2.2.1 Principles of operation of the *Orbitrap* mass analyser (overview)

The principles of operation of the *Orbitrap* can be summarised as follows:

- It exclusively uses an electrostatic field to trap the ions (no RF or magnetic fields).
- Moving ions are trapped around the central electrode with only electrostatic attraction being compensated by centrifugal force (from initial tangential velocity).
- The outer electrode confines ions axially.
- Control of frequencies of oscillation (axial in particular) by shape/geometry of electrodes.

In a very simple way, in this mass analyser, ions are injected tangentially into an electric field between specially shaped electrodes and trapped because their electrostatic attraction to the inner electrode is balanced by centrifugal forces. Thus, ions cycle around the central electrode in rings - rotational motion (elliptical orbiting). In addition, the ions also move back and forth along the axis of the central electrode - axial oscillation. Therefore, ions of a specific mass-to-charge ratio move in rings which oscillate along the central spindle-like electrode. The frequency of these harmonic oscillations is independent of the ion velocity and is inversely proportional to the square root of the mass-to-charge ratio (m/z). By sensing the ion oscillation in a manner similar to that used in FT-ICR (ion image current detection and FFT), the trap can be used as a mass analyser. There are three types of ion trapping linear, segmented and orbital trapping. The latter is the focus of our review.

Orbital trapping (History)

Orbital trapping was first implemented by Kingdon in 1923. (Kingdon 1923) In its classical shape, the Kingdon trap contains a wire stretched along the axis of an outer cylinder with flanges enclosing the trapping volume. When a voltage is applied between the wire and the cylinder, the strong field attracts ions to the wire. Only ions that have sufficient tangential velocity miss the wire and survive. Motion along the wire is restrained by the field curvature caused by the flanges of the outer cylinder. A more elaborate electrode shape has been developed by Knight ("ideal Kingdon trap"). (Knight 1981)

The modified Kingdon trap

Orbital trapping is known to be used in experiments on the spectroscopy of ions. In these applications, ions have been formed within the trap or injected tangentially prior to switching on the field of the trap. (Knight 1981; Lewis 1982; Lisheng and Church 1991; Sekioka, Terasawa et al. 1991)

Makarov (Makarov 2000) proposed the concept of orbital trapping with a fresh review for application to mass analysis. A "new" type of mass analyser was described which employs orbital trapping in an electrostatic field.

For didactic purposes the orbitrap can be considered as an enhanced 'Knight-style' ideal Kingdon trap, but with specially shaped electrodes. When a DC voltage is applied between the two axially symmetric electrodes it results in the electrostatic field with potential distribution described in equation 23.

$$U(r,z) = \frac{k}{2}\left(z^2 - \frac{r^2}{2}\right) + \frac{k}{2}(R_m)^2 \ln\left[\frac{r}{R_m}\right] + C \tag{23}$$

where r and z are cylindrical coordinates (z= 0 being the plane of the symmetry of the field), C is a constant, k is field curvature (or more recently known as axial restoring force determined by the exact shape of the electrodes and applied potential), and R_m is the characteristic radius. For a more detailed description, please refer to literature. (Gillig, Bluhm et al. 1996; Makarov 2000; Makarov, Denisov et al. 2006)

This field, shown in equation (22), is the sum of a quadrupole field of the ion trap (which confines ions axially) and a logarithmic field of a cylindrical capacitor (provides orbital ion trapping); therefore, it is also called a quadro-logarithmic field. It is clear from this expression that there are no cross-terms in r and z, thus motion in z is independent of r, φ-motion (where φ is the angular coordinate).

Geometry of the Orbitrap (axially symmetric electrodes and equations of motion)

The trap consists of an outer barrel-like electrode and a central spindle-like electrode along the axis (see Fig. 10). The geometrical shape of these axially symmetrical electrodes can be deduced from eq. 22:

$$z_{1,2}(r) = \sqrt{\frac{r^2}{2} - \frac{\left(R_{1,2}\right)^2}{2} + (R_m)^2 \ln\left[\frac{R_{1,2}}{r}\right]} \tag{24}$$

where index 1 denotes the central electrode (spindle like), index 2 denotes the outer electrode (with flanges enclosing the trapping volume), z = 0 is the plane of symmetry, and $R_{1,2}$ are the maximum radii of the corresponding electrodes.

Stable ion trajectories involve both orbiting motion around (rotational) the central electrode (r, φ-motion, where φ is the angular coordinate) and simultaneous harmonic oscillations in the z-direction (coherent axial oscillations).

The Ion Trajectories (Equations of motion)

For the *Rotational Motion,* the *r, φ*–motion, although not used for mass analysis, is still important because ions must be trapped in the radial plane. Equilibrium is reached between attraction and centrifugal forces that act on the ions.

For the *Axial Motion*, the movement back and forth around the central electrode, along z, is (approximately) described by a simple harmonic oscillator. The angular frequency of axial oscillations in rad s^{-1} (ω) is defined by equation 25 in terms of the charge (q) and mass (m) of the ion, k the field constant, being essential for establishing the fundamental relation for mass analysis. (Makarov 2000; Hu, Noll et al. 2005; Makarov, Denisov et al. 2006)

$$\omega = \sqrt{(q/m)k} \tag{25}$$

Use of the axial angular frequency as opposed to rotational or radial frequency is critical because only this frequency is completely independent of energy and spatial spread of ions (see below). A mass analyser employing such electrostatic axially harmonic orbital trapping is referred hereinafter as the *Orbitrap*.

This axial frequency may be determined using image current detection and fast FT algorithms. (Dienes, Pastor et al. 1996) The detection of an ion image current due to motion along the *Orbitrap* axis is only possible as long as the ion packets retain their spatial coherence in the axial direction (*i.e.*, phase coherence and small spatial extent). The outer electrode is split in half at $z=0$ allowing the ion image current due to axial motion to be collected. The current is differentially amplified from each half of the outer electrode and then undergoes analog-to-digital conversion before processing and collection by customised control and acquisition software. Transient ion image current in the outer electrodes (split at $z=0$) is acquired as a time-domain transient and transformed to the spectra in the mass spectrometer by applying fast Fourier transform (FFT). The image current is amplified and processed exactly in the same way as in FT ICR; (see previous section) therefore, similar sensitivity and signal-to-noise ratios are expected. The resulting frequency spectrum however differs due to a much slower decrease of ion frequency with mass according to equation 25 when compared with equation 4.

As a conclusion, potential advantages of the *Orbitrap* include:

- high mass resolution (up to 100 000-200 000) since the quadro-logarithmic field (equation 22) may be defined with very high accuracy;
- increased space charge capacity at higher masses due to independence of trapping potential on mass-to-charge ratio and larger trapping volumes in contrast to FT ICR and ion trap;
- high mass accuracy (2-5 ppm internal and external calibration, respectively), dynamic range over which accurate masses can be determined, and upper mass limit;
- high sensitivity and stability; and
- maintenance free analyser (when compared to the FTICR mass analyser where cryogenic liquids or expensive cooling apparatus are needed to maintain the superconducting magnet).

3. Applications

The mass analysers described in this chapter are capable of performing high resolution and high accuracy mass measurements on a routine basis. It is worth mentioning that before such mass analysers were developed, accurate mass measurements were performed only on sector instruments with a great deal of work and time behind each analysis within a restricted mass range (basically the masses in the close vicinity of the measured mass). Nowadays, high resolution can be attained in a broad mass range and the spectra are acquired in a couple of minutes (usually the time spent to acquire an HR mass spectrum is well below 1 minute).

To demonstrate how useful high resolution is, electrospray ionisation (ESI) mass spectra will be shown that were acquired on two different instruments: an Apex Ultra FTICR mass spectrometer equipped with a 7 T superconducting magnet (Bruker Daltonics, Bremen, Germany) and a LCQ-Duo ion trap mass spectrometer (Thermo Fisher Scientific, Bremen Germany). The high- and low-resolution ESI mass spectra of ubiquitin are depicted in Fig. 12. Even though both systems provide information about charge state distribution, it is perfectly clear that the isotopic envelope is completely resolved when using an FTICR system (see insets in Fig. 12).

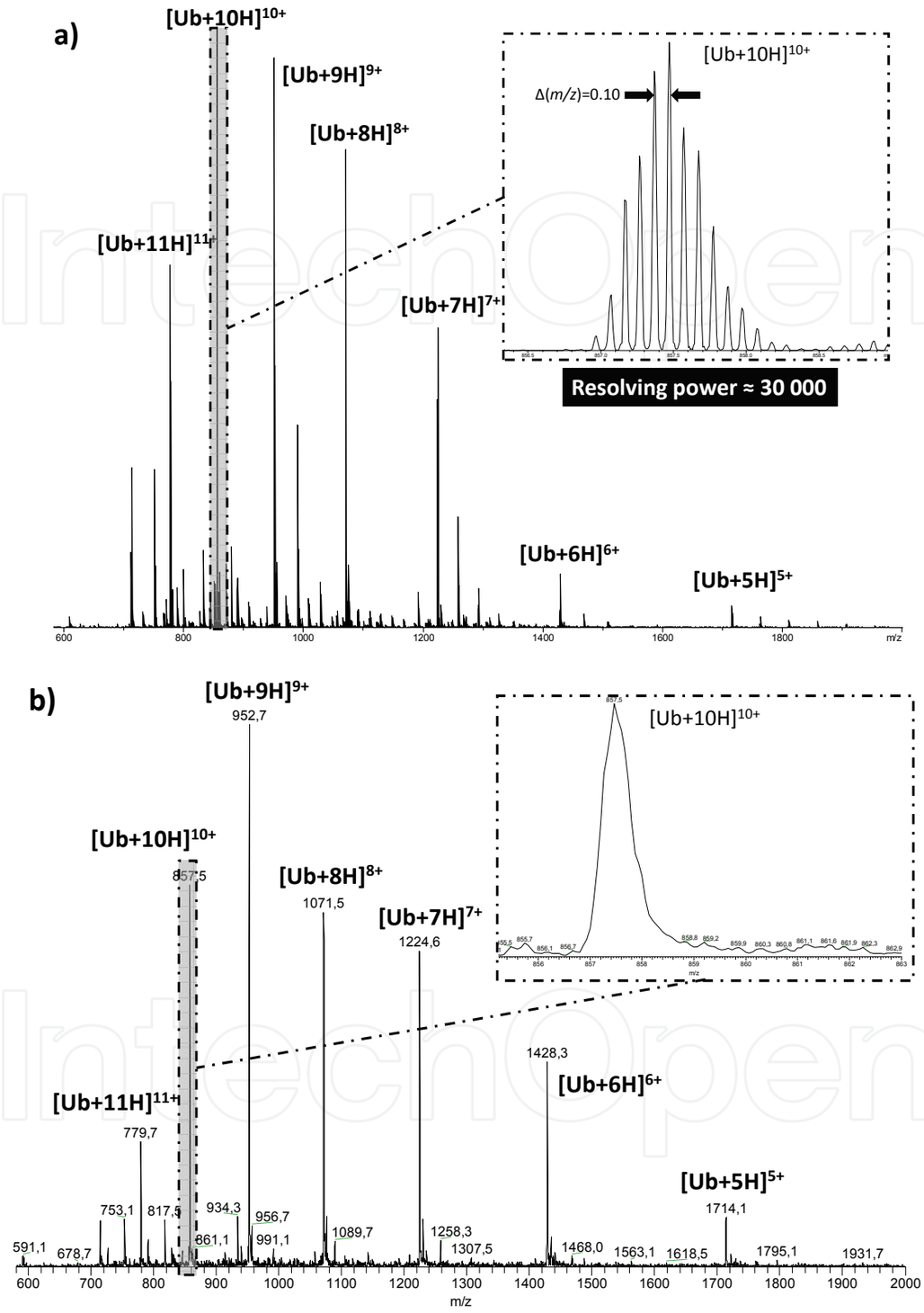

Fig. 12. High resolution (a) and low resolution (b) electrospray ionisation mass spectra of Ubiquitin (Ub). The insets show an expansion of the peak at *m/z* 857.5 attributed to $[Ub+10H]^{10+}$ ion. (High resolution system: 7 T Apex Ultra FTICR-MS from Bruker Daltonics; Low resolution system LCQ-Duo ion trap mass spectrometer from Thermo Fisher Scientific

There are basically two ways to determine the charge state of a given ion. One involves the analysis of the isotope envelope, implying that it can only be used in high-resolution mass spectrometry, while the other relates each peak with the subsequent one and can be used in high- and low-resolution mass spectrometry.

The mass difference between two isotopic peaks is related to the charge state by $z=1/\Delta(m/z)$, hence, for the ubiquitin ion at m/z 857.47 ($[Ub+10H]^{10+}$ ion of Fig. 12a) the charge state will be given by $z= (1/0.10) = 10$. It is worth mentioning that isotopic peaks are useful in the interpretation as long as there is no interference from other ions.

Considering that two adjacent peaks in the mass spectrum, for example, m/z 857.5 and m/z 957.7 of Fig. 12b, are due to the same entity (i.e. they reflect different charge states of ubiquitin), one can assume that $m = 857.5z'$ and $m = 957.7z$ (where $z' = z+1$), i.e. $857.5 (z+1) = 957.7z$, hence $z = 9$. As such the ion at m/z 957.7 corresponds to a 9+ ion while the ion at m/z 857.5 corresponds to a 10+ ion.

4. Acknowledgments

The authors acknowledge the funding provided by Fundação para a Ciência e a Tecnologia (PEst-OE/QUI/UI0612/2011 and REDE/1501/REM/2005). Pedro A. Alves acknowledges Fundação para a Ciência e a Tecnologia for the PhD grant (SFRH/BD/49069/2008). Thermo Fisher Scientific and Dr. Michaela Scigelova are gratefully acknowledged for supplying the *Orbitrap* images.

5. References

Aston, F. W. (1919). *LXXIV. A positive ray spectrograph*. Philosophical Magazine Series 6 38 (228): 707 - 714.

Bainbridge, K. T. (1932). *The isotopic weight of H_2*. Physical Review 42 (1): 1-10.

Bainbridge, K. T. and E. B. Jordan (1936). *Mass spectrum analysis 1. The mass spectrograph. 2. The existence of isobars of adjacent elements*. Physical Review 50 (4): 282-296.

Barber, M., R. S. Bordoli, et al. (1981). *Fast atom bombardment of solids (F.A.B.): a new ion source for mass spectrometry*. Journal of the Chemical Society, Chemical Communications (7): 325-327.

Comisarow, M. B. and A. G. Marshall (1974). *Fourier transform ion cyclotron resonance spectroscopy*. Chemical Physics Letters 25 (2): 282-283.

Covey, T. R., E. C. Huang, et al. (2002). *Structural characterization of protein tryptic peptides via liquid chromatography/mass spectrometry and collision-induced dissociation of their doubly charged molecular ions*. Analytical Chemistry 63 (13): 1193-1200.

Dass, C. (2007). *Fundamentals of Contemporary Mass Spectrometry*. Hoboken, New Jersey, John Wiley & Sons.

Dempster, A. J. (1918). *A new method of positive ray analysis*. Physical Review 11 (4): 316-325.

Dienes, T., S. J. Pastor, et al. (1996). *Fourier transform mass spectrometry - advancing years (1992–mid. 1996)*. Mass Spectrometry Reviews 15 (3): 163-211.

Fenn, J. B., M. Mann, et al. (1989). *Electrospray ionization for mass spectrometry of large biomolecules*. Science 246 (4926): 64-71.

Gillig, K. J., B. K. Bluhm, et al. (1996). *Ion motion in a Fourier transform ion cyclotron resonance wire ion guide cell*. International Journal of Mass Spectrometry and Ion Processes 157-158: 129-147.

Gross, J. H. (2004). *Mass Spectrometry: A Textbook*. Berlin, Springer-Verlag.

Hager, J. W. (2002). *A new linear ion trap mass spectrometer*. Rapid Communications in Mass Spectrometry 16 (6): 512-526.

Heeren, R. M. A., A. J. Kleinnijenhuis, et al. (2004). *A mini-review of mass spectrometry using high-performance FTICR-MS methods*. Analytical and Bioanalytical Chemistry 378 (4): 1048-1058.

Hoffmann, E. d. and V. Stroobant (2007). *Mass spectrometry: Principles and Applications*. Chichester, John Wiley & Sons.

Hu, Q., R. J. Noll, et al. (2005). *The Orbitrap: a new mass spectrometer*. Journal of Mass Spectrometry 40 (4): 430-443.

Jennings, K. R. (1968). *Collision-induced decompositions of aromatic molecular ions*. International Journal of Mass Spectrometry and Ion Physics 1 (3): 227-235.

Johnson, E. G. and A. O. Nier (1953). *Angular aberrations in sector shaped electromagnetic lenses for focusing beams of charged particles*. Physical Review 91 (1): 10-17.

Jung, H. R., D. Pasini, et al. (2010). *Quantitative mass spectrometry of Histones H3.2 and H3.3 in Suz12-deficient mouse embryonic stem cells reveals distinct, dynamic post-translational modifications at Lys-27 and Lys-36*. Molecular & Cellular Proteomics 9 (5): 838-850.

Karas, M. and F. Hillenkamp (2002). *Laser desorption ionization of proteins with molecular masses exceeding 10,000 daltons*. Analytical Chemistry 60 (20): 2299-2301.

Kingdon, K. H. (1923). *A method for the neutralization of electron space charge by positive ionization at very low gas pressures*. Physical Review 21 (4): 408-418.

Knight, R. D. (1981). *Storage of ions from laser-produced plasmas*. Applied Physics Letters 38 (4): 221-223.

Lewis, R. R. (1982). *Motion of ions in the Kingdon trap*. Journal of Applied Physics 53 (6): 3975-3980.

Lisheng, Y. and D. A. Church (1991). *Confinement of injected beam ions in a Kingdon trap*. Nuclear Instruments and Methods in Physics Research Section B: Beam Interactions with Materials and Atoms 56-57, Part 2: 1185-1187.

Makarov, A. (2000). *Electrostatic axially harmonic orbital trapping: a high-performance technique of mass analysis*. Analytical Chemistry 72 (6): 1156-1162.

Makarov, A., E. Denisov, et al. (2006). *Performance evaluation of a hybrid linear ion trap/Orbitrap mass spectrometer*. Analytical Chemistry 78 (7): 2113-2120.

Marshall, A. G., M. B. Comisarow, et al. (1979). *Relaxation and spectral line shape in Fourier transform ion resonance spectroscopy*. Journal of Chemical Physics 71 (11): 4434-4444.

Marshall, A. G., C. L. Hendrickson, et al. (1998). *Fourier transform ion cyclotron resonance mass spectrometry: A primer*. Mass Spectrometry Reviews 17 (1): 1-35.

Marshall, A. G. and F. R. Verdun (1990). *Fourier tansforms in NMR, optical, and mass spectrometry: a user's handbook.* New York, Elsevier.

Munson, M. S. B. and F. H. Field (1966). *Chemical ionization mass spectrometry. I. General Introduction*. Journal of the American Chemical Society 88 (12): 2621-2630.

Nier, A. O. (1940). *A mass Spectrometer for routine isotope abundance measurements*. Review of Scientific Instruments 11 (7): 212-216.

Paul, W. (1990). *Electromagnetic traps for charged and neutral particles*. Reviews of Modern Physics 62 (3): 531-540.

Perry, R. H., R. G. Cooks, et al. (2008). *Orbitrap mass spectrometry: Instrumentation, ion motion and applications*. Mass Spectrometry Reviews 27 (6): 661-699.

Rodrigues, J. A., A. M. Taylor, et al. (2007). *Mass Spectrometry of Carbohydrates: Newer Aspects*, In *Advances in Carbohydrate Chemistry and Biochemistry*. D. Horton. London, Academic Press. Volume 61: 59-141.

Ryhage, R. (2002). *Use of a mass spectrometer as a detector and analyzer for effluent emerging from high temperature gas liquid chromatography columns*. Analytical Chemistry 36 (4): 759-764.

Sekioka, T., M. Terasawa, et al. (1991). *Ion storage in Kingdon trap*. Radiation Effects and Defects in Solids 117 (1-3): 253-259.

Sommer, H., H. A. Thomas, et al. (1951). *The measurement of e/M by cyclotron resonance*. Physical Review 82 (5): 697-702.

Thomson, J. J. (1897). *Cathode rays*. Philosophical Magazine Series 5 44 (269): 293-316.

Thomson, J. J. (1907). *On rays of positive electricity*. Philosophical Magazine Series 6 13 (77): 561-575.

Vartanian, V. H., J. S. Anderson, et al. (1995). *Advances in trapped ion cells for Fourier transform ion cyclotron resonance mass spectrometry*. Mass Spectrometry Reviews 14 (1): 1-19.

Voyksner, R. D. (1997). *Combining Liquid Chromatography with Electrospray Mass Spectrometry*, In *Electrospray Ionization Mass Spectrometry: Fundamentals, Instrumentation, and Applications*. R. B. Cole. New York, John Wiley & Sons: 323-342.

Watson, J. T. and K. Biemann (2002). *Direct recording of high resolution mass spectra of gas chromatographic effluents*. Analytical Chemistry 37 (7): 844-851.

Whitehouse, C. M., R. N. Dreyer, et al. (2002). *Electrospray interface for liquid chromatographs and mass spectrometers*. Analytical Chemistry 57 (3): 675-679.

Wolff, M. M. and W. E. Stephens (1953). *A pulsed mass spectrometer with time dispersion*. Review of Scientific Instruments 24 (8): 616-617.

Zhang, L.-K., D. Rempel, et al. (2005). *Accurate mass measurements by Fourier transform mass spectrometry*. Mass Spectrometry Reviews 24 (2): 286-309.

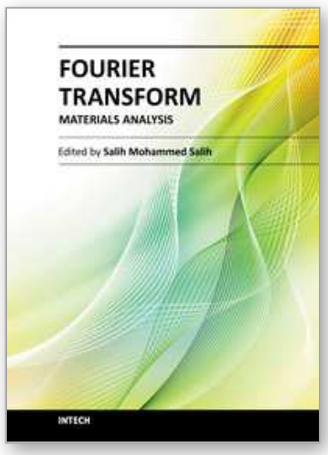

Fourier Transform - Materials Analysis

Edited by Dr Salih Salih

ISBN 978-953-51-0594-7

Hard cover, 260 pages

Publisher InTech

Published online 23, May, 2012

Published in print edition May, 2012

The field of material analysis has seen explosive growth during the past decades. Almost all the textbooks on materials analysis have a section devoted to the Fourier transform theory. For this reason, the book focuses on the material analysis based on Fourier transform theory. The book chapters are related to FTIR and the other methods used for analyzing different types of materials. It is hoped that this book will provide the background, reference and incentive to encourage further research and results in this area as well as provide tools for practical applications. It provides an applications-oriented approach to materials analysis written primarily for physicist, Chemists, Agriculturalists, Electrical Engineers, Mechanical Engineers, Signal Processing Engineers, and the Academic Researchers and for the Graduate Students who will also find it useful as a reference for their research activities.

INTECH
open science | open minds

InTech Europe
University Campus STeP Ri
Slavka Krautzeka 83/A
51000 Rijeka, Croatia
Phone: +385 (51) 770 447
Fax: +385 (51) 686 166
www.intechopen.com

InTech China
Unit 405, Office Block, Hotel Equatorial Shanghai
No.65, Yan An Road (West), Shanghai, 200040, China
中国上海市延安西路65号上海国际贵都大饭店办公楼405单元
Phone: +86-21-62489820
Fax: +86-21-62489821

IntechOpen